An extended cyclic plasticity model at finite deformations describing the Bauschinger effect and ratchetting behaviour

Yilin Zhu [1], Guozheng Kang [1,*], Qianhua Kan [1], Chao Yu [1]
Jun Ding [1]

[1] Department of Applied Mechanics and Engineering, Southwest Jiaotong University, Chengdu, 610031, China
* Corresponding author: Guozhengkang@126.com

Abstract A popular cyclic plasticity model at small deformations is extended to finite deformations for describing the Bauschinger effect and ratchetting behaviour by considering the combined isotropic and kinematic hardening rules. The model is based on the multiplicative decomposition of deformation gradient into elastic and inelastic parts. Following, a further multiplicative decomposition of inelastic part of deformation gradient into energetic and dissipative parts is adopted to extend the popular Ohno-Karim nonlinear kinematic hardening rule. Finally, numerical examples are carried out to validate the proposed model under strain controlled and stress controlled cyclic loadings.

Keywords Finite deformation, cyclic plasticity, ratchetting; kinematic hardening, Bauschinger effect

1. Introduction

In engineering applications, engineering components are usually subjected to complex cyclic loading. For instance, metal forming, mechanical cutting, wheel/rail contact in high speed railway and aero fasteners connection, etc. Cyclic plasticity models for describing Bauschinger effect and ratchetting behaviour of metals associated with cyclic loading have been one of the most popular research topic for solid mechanics in recent years. At small deformation regime, cyclic constitutive model research has reaped great achievements under the effort of numerous scholars [1-9]. The most popular model, which can describe Bauschinger effect and ratchetting behaviour, is Armstrong-Frederick kinematic model (shorted as A-F model) [1]. Even though the prediction of ratchetting behaviour by A-F model is too high relative to the actual situation, it is still widely applied in engineering analysis due to its solid physical background and concise theory system. And after then, there have been a lot of attempts to modify A-F model to improve predicting in ratcheting [2-9]. Ohno-Karim model, owing to the convenience of material parameters determination and the reasonable prediction in ratchetting, was widely adopted to simulate cyclic plastic behaviour of metal materials at present. The models were mostly constructed in the frame of small deformation.

It is must be noted that the deformation of structural components is finite and associated with finite rotation in practical modelling situations.. Cyclic constitutive models established at small deformation regime are no longer suitable for these circumstances due to without considering rotation effect. Recently, some constitutive models were extended from small deformation to finite deformation [10-24]. Among these models, two main strategies are followed. One class is hypo-elasticity theory which is developed by introducing a stress-like internal variable to model

kinematic hardening with the assumption that the stretching tensor is additively decomposed into the elastic part and plastic part. This theory requires adopting appropriate objective stress rate to establish the frame-indifference evolution equations. Alternatively, the other one is hyper-elasticity theory, in which the inelastic part is based on the standard Kröner multiplicative decomposition [25] and can be further multiplicatively decomposed into energetic and dissipative parts [15]. In hyper-elasticity theory, a strain-like internal variable is introduced to model kinematic hardening. The requirement of this strategy is to establish all evolution equations in the same configuration. For the first strategy, it has been shown that the rate form model for elastic response is integrable [18, 26] only in form of the logarithmic rate. Therefore, some unreasonable responses in elastic behaviour, such as shear oscillatory phenomenon and the nonzero work in a hysteretic loop, may appear. To avoid the nonzero work in elastic response, a continuum mechanical extension of A-F type kinematic hardening rule can be achieved naturally motivated by a typical rheological model description. However, as so far only A-F model is extended in both of the two strategies.

In the present work, the Ohno-Karim model is firstly extended from small deformations to finite deformations based on the hyper-elasticity theory. Some numerical examples were provided to display the prediction in Bauschinger effect and ratchetting behaviour under strain controlled and stress controlled cyclic loadings, respectively.

2. Continuum extension of Ohno-Karim model at finite deformations

2.1. Kinematic

In order to model the inelastic response of materials, the deformation gradient $\mathbf{F}$ may be classically multiplicatively decomposed as

$$\mathbf{F} = \mathbf{F}^e\mathbf{F}^p \tag{1}$$

where, $\mathbf{F}^p$ represents the local inelastic distortion of material due to “plastic mechanism”, and this local deformation carries the material from reference space ($\tilde{\mathrm{K}}$) to structure space ($\hat{\mathrm{K}}$); $\mathbf{F}^e$ represents the subsequent stretching and rotation, and it maps material element from structure space ($\hat{\mathrm{K}}$) to current space (K) (see Fig. 1) [25].

Following, $\mathbf{F}^p$ can be further multiplicatively decomposed into energetic part $\mathbf{F}^{pe}$ and dissipative part $\mathbf{F}^{pi}$ [15].

$$\mathbf{F}^p = \mathbf{F}^{pe}\mathbf{F}^{pi} \tag{2}$$

where, $\mathbf{F}^{pi}$ maps material element from reference space into intermediate configuration of kinematic hardening($\breve{\mathrm{K}}$); and $\mathbf{F}^{pe}$ maps material element from intermediate configuration($\breve{\mathrm{K}}$) into structure space(K) (see Fig. 4) [15, 24].
Three right Cauchy-Green tensors are given by

$$\mathbf{C} = \mathbf{F}^T\mathbf{F}, \quad \mathbf{C}^e = \mathbf{F}^{eT}\mathbf{F}^e = \mathbf{F}^{p-T}\mathbf{C}\mathbf{F}^{p-1}, \quad \mathbf{C}^{pe} = \mathbf{F}^{peT}\mathbf{F}^{pe} = \mathbf{F}^{pi-T}\mathbf{C}^p\mathbf{F}^{pi-1} \tag{3}$$

with

$$\mathbf{C}^p = \mathbf{F}^{pT}\mathbf{F}^p \tag{4}$$

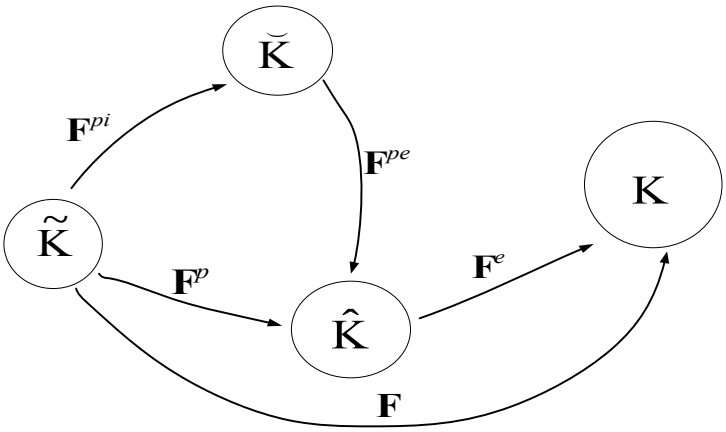

Figure 1. Elastic-inelastic decomposition of the kinematics deformation

2.2. Helmholtz free energy

Similar to the small deformation regime and based on the requirement of material objectivity, the Helmholtz free energy is additively decomposed into three parts

$$\psi = \psi^{e}\left(\mathbf{C}^{e}\right) + \psi^{kin}\left(\mathbf{C}^{pe}\right) + \psi^{iso}\left(p\right) \tag{5}$$

where ψ^{e} represents the standard energy associated with intermolecular interactions; ψ^{kin} is a defect-energy associated with plastic deformation; and $\psi^{iso}\left(p\right)$ represents the additional amount of stored energy related to isotropic hardening, where p is accumulated plastic strain.

2.3. Clausius-Duhem inequality

Inspired by the existing work [21, 23], we derive the constitutive equations of Ohno-Karim model in a continuum method in this paper. The derivation is based on the requirement of the Clausius-Duhem inequality.

For isothermal process, the reduced Clausius-Duhem inequality is

$$\mathbf{S} : \frac{1}{2}\dot{\mathbf{C}} - \dot{\psi} \geq 0 \tag{6}$$

where $\mathbf{S}$ is the second Piola-Kirchhoff stress tensor; $(:)$ represents the inner product of tensors.

For Ohno-Karim kinematic hardening rule, the kinematic free energy term is given by

$$\psi^{kin} = \sum_{i}^{N} \psi_{i}^{kin}\left(\mathbf{C}_{i}^{pe}\right)\left(N \geq 1\right) \tag{7}$$

with

$$\mathbf{C}_{i}^{pe} = \mathbf{F}_{i}^{pe^{T}}\mathbf{F}_{i}^{pe} \tag{8}$$

and

$$\mathbf{F}_{i}^{pe} = \mathbf{F}^{p}\mathbf{F}_{i}^{pi^{-1}} \tag{9}$$

Eq. (9) indicates that the form of multiplicative decomposition for $\mathbf{F}^{p}$ is not exclusive.

Combing Eq. (7) and Eq. (5), yields

$$\psi = \psi^{e}\left(\mathbf{C}^{e}\right) + \sum_{i}^{N} \psi_{i}^{kin}\left(\mathbf{C}_{i}^{pe}\right) + \psi^{iso}\left(p\right) \tag{10}$$

Substituting Eq. (10) into Eq. (6), the Clausius-Duhem inequality can be rewritten as

$$\mathbf{S}:\frac{1}{2}\dot{\mathbf{C}}-\frac{\partial\psi^{e}}{\partial\mathbf{C}^{e}}:\dot{\mathbf{C}}^{e}-\sum_{i}^{N}\frac{\partial\psi_{i}^{kin}}{\partial\mathbf{C}_{i}^{pe}}:\dot{\mathbf{C}}_{i}^{pe}-\frac{\partial\psi^{iso}}{\partial p}\dot{p}\geq 0 \tag{11}$$

According Eq. (3),

$$\dot{\mathbf{C}}^{e}=\dot{\mathbf{F}}^{p^{-T}}\mathbf{C}\mathbf{F}^{p^{-1}}+\mathbf{F}^{p^{-T}}\dot{\mathbf{C}}\mathbf{F}^{p^{-1}}+\mathbf{F}^{p^{-T}}\mathbf{C}\dot{\mathbf{F}}^{p^{-1}} \tag{12}$$

Furthermore, by adopting the two identities, gives

$$\dot{\mathbf{F}}^{p^{-1}}=-\mathbf{F}^{p^{-1}}\dot{\mathbf{F}}^{p}\mathbf{F}^{p^{-1}},\quad \dot{\mathbf{F}}^{p^{-T}}=-\mathbf{F}^{p^{-T}}\dot{\mathbf{F}}^{p}\mathbf{F}^{p^{-T}} \tag{13}$$

Combing Eq. (12) and Eq. (13), $\dot{\mathbf{C}}^{e}$ is derived as

$$\dot{\mathbf{C}}^{e}=-\mathbf{L}^{p^{T}}\mathbf{C}^{e}+\mathbf{F}^{p^{-T}}\dot{\mathbf{C}}\mathbf{F}^{p^{-1}}-\mathbf{C}^{e}\mathbf{L}^{p} \tag{14}$$

where $\mathbf{L}^{p}=\dot{\mathbf{F}}^{p}\mathbf{F}^{p^{-1}}$ is the plastic velocity gradient.

In the same process,

$$\dot{\mathbf{C}}_{i}^{pe}=-\mathbf{L}_{i}^{pi^{T}}\mathbf{C}_{i}^{pe}+\mathbf{F}_{i}^{pi^{-T}}\dot{\mathbf{C}}^{p}\mathbf{F}_{i}^{pi^{-1}}-\mathbf{C}_{i}^{pe}\mathbf{L}_{i}^{pi} \tag{15}$$

where $\mathbf{L}_{i}^{pi}=\dot{\mathbf{F}}_{i}^{pi}\mathbf{F}_{i}^{pi^{-1}}$ is the so called "inelastic" plastic velocity gradient.

Considering the symmetric property of tensor functions ψ^{e} and ψ_{i}^{kin} [23]

$$\frac{\partial\psi^{e}}{\partial\mathbf{C}^{e}}:\left(\mathbf{C}^{e}\mathbf{L}^{p}\right)=\left(\mathbf{C}^{e}\frac{\partial\psi^{e}}{\partial\mathbf{C}^{e}}\right):\mathbf{D}^{p} \tag{16a}$$

$$\frac{\partial\psi_{i}^{kin}}{\partial\mathbf{C}_{i}^{pe}}:\left(\mathbf{C}_{i}^{pe}\mathbf{L}_{i}^{pi}\right)=\left(\mathbf{C}_{i}^{pe}\frac{\partial\psi_{i}^{kin}}{\partial\mathbf{C}_{i}^{pe}}\right):\mathbf{D}_{i}^{pi} \tag{16b}$$

where $\mathbf{D}^{p}$ and $\mathbf{D}_{i}^{pi}$ are symmetric part of $\mathbf{L}^{p}$ and $\mathbf{L}_{i}^{pi}$, respectively.

Moreover

$$\mathbf{D}^{p}=\frac{1}{2}\mathbf{F}^{p^{-T}}\dot{\mathbf{C}}\mathbf{F}^{p^{-1}},\quad \mathbf{D}_{i}^{pi}=\mathbf{F}_{i}^{pi^{-T}}\dot{\mathbf{C}}^{p}\mathbf{F}_{i}^{pi^{-1}} \tag{17}$$

By Eqs. (14)- (17), the Clausius-Duhem inequality (11) yields the final form

$$\begin{aligned}&\left(\mathbf{S}-2\mathbf{F}^{p^{-1}}\frac{\partial\psi^{e}}{\partial\mathbf{C}^{e}}\mathbf{F}^{p^{-T}}\right):\frac{1}{2}\dot{\mathbf{C}}+\left(2\mathbf{C}^{e}\frac{\partial\psi^{e}}{\partial\mathbf{C}^{e}}-2\sum_{i}^{N}\mathbf{F}_{i}^{pe}\frac{\partial\psi_{i}^{kin}}{\partial\mathbf{C}_{i}^{pe}}\mathbf{F}_{i}^{pe^{T}}\right):\mathbf{D}^{p}\\&+2\sum_{i}^{N}\left(\mathbf{C}_{i}^{pe}\frac{\partial\psi_{i}^{kin}}{\partial\mathbf{C}_{i}^{pe}}:\mathbf{D}_{i}^{pi}\right)-\frac{\partial\psi^{iso}}{\partial p}\dot{p}\geq 0\left(N\geq 1\right)\end{aligned} \tag{18}$$

According to the Coleman-Noll procedure, the second Piola-Kirchhoff stress tensor can be defined as

$$\mathbf{S}=2\mathbf{F}^{p^{-1}}\frac{\partial\psi^{e}}{\partial\mathbf{C}^{e}}\mathbf{F}^{p^{-T}} \tag{19}$$

Furthermore, the so-called Mandel stress $\mathbf{M}$, kinematic Mandel stress $\mathbf{M}^{kin}$, back stress $\boldsymbol{\chi}$ and isotropic deformation resistance *R* are defined as follows:

$$\mathbf{M}=2\mathbf{C}^{e}\frac{\partial\psi^{e}}{\partial\mathbf{C}^{e}} \tag{20}$$

and

$$\mathbf{M}^{kin}=\sum_{i}^{N}\mathbf{M}_{i}^{kin} \tag{21}$$

with

$$\mathbf{M}_i^{kin} = 2\mathbf{C}_i^{pe}\frac{\partial \psi_i^{kin}}{\partial \mathbf{C}_i^{kin}} \tag{22}$$

and

$$\boldsymbol{\chi} = \sum_i^N \boldsymbol{\chi}_i \tag{23}$$

with

$$\boldsymbol{\chi}_i = 2\mathbf{F}_i^{pe}\frac{\partial \psi_i^{kin}}{\partial \mathbf{C}_i^{pe}}\mathbf{F}_i^{peT} \tag{24}$$

and

$$R = -\frac{\partial \psi^{iso}}{\partial p} \tag{25}$$

In general, R can be written in the Voce's exponential form

$$R = Q\left(1-\exp(-bp)\right) \tag{26}$$

where Q and b are nonnegative material parameters.

Finally, the Clausius-Duhem inequality reduces to the form

$$\left(\mathbf{M}-\boldsymbol{\chi}\right):\mathbf{D}^p + \sum_i^N \mathbf{M}_i^{kin}:\mathbf{D}_i^{pi} + R\dot{p} \geq 0 \tag{27}$$

The evolution equations of Ohno-Karim model can be given by

$$\mathbf{D}^p = \dot{\lambda}\frac{\partial F_y}{\partial \mathbf{M}} = \dot{\lambda}\frac{\mathbf{M}^D-\boldsymbol{\chi}}{\left\|\mathbf{M}^D-\boldsymbol{\chi}\right\|} \tag{28a}$$

$$\mathbf{D}_i^{pi} = u_i b_i \dot{\lambda}\mathbf{M}_i^{kin} + H\left(f_i\right)\frac{b_i}{c_i}\mathbf{M}_i^{kin}\left\langle \mathbf{D}^p:\mathbf{K}_i - u_i\dot{\lambda}\right\rangle \tag{28b}$$

$$\dot{p} = \sqrt{\frac{2}{3}}\dot{\lambda} \tag{28c}$$

with the yield function

$$F_y = \left\|\mathbf{M}^D-\boldsymbol{\chi}\right\| - \sqrt{\frac{2}{3}}\left(\sigma_y + R\right) \tag{29}$$

where the superscript D denotes the deviator of a tensor, i.e. $\mathbf{A}^D = \mathbf{A} - \frac{1}{3}tr\left(\mathbf{A}\right)\mathbf{1}$.

and the plastic multiplier $\dot{\lambda}$ is determined by the Kuhn-Tucker conditions

$$\dot{\lambda} \geq 0\,, \quad F_y \leq 0\,, \quad \dot{\lambda}F_y = 0\left(if\ F_y = 0\right) \tag{30}$$

In Eq. (28b), b_i and c_i are nonnegative kinematic parameters; H and $\left\langle\ \right\rangle$ are Heaviside function and Macauley operator, respectively; f_i represents the critical surface for i-th back stress which is defined by

$$f_i = \left\|\boldsymbol{\chi}_i\right\|^2 - \left(\frac{c_i}{b_i}\right)^2 \tag{31}$$

And forther more

$$\mathbf{K}_i = \frac{\boldsymbol{\chi}_i}{\left\|\boldsymbol{\chi}_i\right\|} \tag{32}$$

By the foregoing equations

$$
\begin{aligned}
&(\mathbf{M}-\boldsymbol{\chi}):\mathbf{D}^p+\sum_i^N \mathbf{M}_i^{kin}:\mathbf{D}_i^{pi}+R\dot{p}\\
&=\dot{\lambda}\left\|\mathbf{M}^D-\boldsymbol{\chi}\right\|+\dot{\lambda}\sum_i^N\left(u_i b_i+H(f_i)\frac{b_i}{c_i}\left\langle \mathbf{D}^p:\mathbf{K}_i-u_i\dot{\lambda}\right\rangle\right)\left\|\mathbf{M}_i^{kin}\right\|^2+R\sqrt{\frac{2}{3}}\dot{\lambda} \qquad (33)\\
&=\dot{\lambda}\left(F_y+\sqrt{\frac{2}{3}}\sigma_y\right)+\dot{\lambda}\sum_i^N\left(u_i b_i+H(f_i)\frac{b_i}{c_i}\left\langle \mathbf{D}^p:\mathbf{K}_i-u_i\dot{\lambda}\right\rangle\right)\left\|\mathbf{M}_i^{kin}\right\|^2
\end{aligned}
$$

Based on the foregoing statement, Eq. (33) is nonnegative can be obtained directly. Thus, the Clausius-Duhem inequality is satisfied.

However, it should be noted that the constitutive equations (19), (28) and (29) are not defined in the same configuration. The second Piola-Kirchhoff stress (Eq. (19)) is defined in the reference configuration; Eqs. (28a) and (28b) act in the structure configuration and the intermediate configuration of kinematic hardening, respectively; Eqs. (28c) and (29) are scalar equations [23]. In order to satisfy the basic requirement of constitutive model, the evolution equations (28a) and (28b) are transformed to the reference configuration, in the following. Obviously, the yield function is also rewritten in term of quantities defined in the reference configuration.

2.4. Representation in the reference configuration

It has been proved that the second Piola-Kirchhoff stress tensor is only the function of $\mathbf{C}$ and $\mathbf{C}^p$ [23], namely

$$\mathbf{S}=\tilde{\mathbf{S}}\left(\mathbf{C},\mathbf{C}^p\right) \qquad (34)$$

A new back stress tensor $\mathbf{X}_i$ defined as a pullback of $\boldsymbol{\chi}_i$ by $\mathbf{F}_i^p$, i.e.

$$\mathbf{X}_i=\mathbf{F}_i^{p^{-1}}\boldsymbol{\chi}_i\mathbf{F}_i^{p^{-T}}=2\mathbf{F}_i^{p^{-1}}\mathbf{F}_i^{pe}\frac{\partial\psi_i^{kin}}{\partial\mathbf{C}_i^{pe}}\mathbf{F}_i^{pe^T}\mathbf{F}_i^{p^{-T}}=2\mathbf{F}_i^{pi^{-1}}\frac{\partial\psi_i^{kin}}{\partial\mathbf{C}_i^{pe}}\mathbf{F}_i^{pi^{-T}} \qquad (35)$$

also is the function of $\mathbf{C}^p$ and $\mathbf{C}_i^{pi}$ only [23], namely

$$\mathbf{X}_i=\tilde{\mathbf{X}}_i\left(\mathbf{C}^p,\mathbf{C}_i^{pi}\right) \qquad (36)$$

It means that the back stress tensor $\mathbf{X}_i$ is defined in the reference configuration. Then, the total back stress is

$$\mathbf{X}=\sum_i^N\mathbf{X}_i \qquad (37)$$

Further, according to Eq. (17), it can be obtained that

$$\dot{\mathbf{C}}^p=2\mathbf{F}^{p^T}\mathbf{D}^p\mathbf{F}^p,\quad \dot{\mathbf{C}}_i^{pi}=\mathbf{F}_i^{pi^T}\mathbf{D}_i^{pi}\mathbf{F}_i^{pi} \qquad (38)$$

Thus, the evolution of $\dot{\mathbf{C}}^p$ and $\dot{\mathbf{C}}_i^{pi}$ have the form

$$\dot{\mathbf{C}}^p=2\dot{\lambda}\mathbf{F}^{p^T}\frac{\mathbf{M}^D-\boldsymbol{\chi}}{\left\|\mathbf{M}^D-\boldsymbol{\chi}\right\|}\mathbf{F}^p=2\dot{\lambda}\frac{\mathbf{Y}^D\mathbf{C}^p}{\sqrt{\mathbf{Y}^D:\mathbf{Y}^D}} \qquad (39a)$$

$$
\begin{aligned}
\dot{\mathbf{C}}_i^{pi}&=2\mathbf{F}_i^{pi^T}\left(u_i b_i\dot{\lambda}\mathbf{M}_i^{kin}+H(f_i)\frac{b_i}{c_i}\mathbf{M}_i^{kin}\left\langle \mathbf{D}^p:\mathbf{K}_i-u_i\dot{\lambda}\right\rangle\right)\mathbf{F}_i^{pi}\\
&=2\dot{\lambda}\left(u_i b_i+H(f_i)\frac{b_i}{c_i}\left\langle \mathbf{D}^p:\mathbf{K}_i-u_i\dot{\lambda}\right\rangle\right)\mathbf{Y}_i^{kin}\mathbf{C}_i^{pi}
\end{aligned} \qquad (39b)
$$

with

$$\mathbf{Y}=\mathbf{CS}-\mathbf{C}^{p}\mathbf{X}=\tilde{\mathbf{Y}}\left(\mathbf{C},\mathbf{C}^{p},\mathbf{C}_{i}^{pi}\right),\quad \mathbf{Y}_{i}^{kin}=\mathbf{C}^{p}\mathbf{X}_{i}=\tilde{\mathbf{Y}}_{i}^{kin}\left(\mathbf{C}^{p},\mathbf{C}_{i}^{pi}\right) \tag{40}$$

and

$$f_{i}=\left\|\boldsymbol{\chi}_{i}\right\|^{2}-\left(\frac{c_{i}}{b_{i}}\right)^{2},\quad \mathbf{K}_{i}=\frac{\boldsymbol{\chi}_{i}}{\left\|\boldsymbol{\chi}_{i}\right\|} \tag{41}$$

Clearly, all constitutive equations are represented in terms of the symmetric tensor $\mathbf{C}$, $\mathbf{C}^{p}$ and $\mathbf{C}_{i}^{pi}$ and the plastic multiplier $\dot{\lambda}$. And the yield function is

$$F_{y}=\sqrt{\mathbf{Y}^{D}:\mathbf{Y}^{D}}-\sqrt{\frac{2}{3}}\left(\sigma_{y}+R\right) \tag{42}$$

Kuhn-Tucker conditions are as following

$$\dot{\lambda}\geq 0,\quad F_{y}\leq 0,\quad \dot{\lambda}F_{y}=0\left(if\ F_{y}=0\right) \tag{43}$$

For numerical examples to be discussed in the follow section, the specific form of the second Piola-Kirchhoff stress and back stress can be given by the well-known neo-Hookean form [23], i.e.

$$\psi^{e}=\frac{\mu}{2}\left(tr\mathbf{C}^{e}-3\right)-\mu\ln\left(\sqrt{\det\mathbf{C}^{e}}\right)+\frac{\Lambda}{4}\left(\det\mathbf{C}^{e}-1-2\ln\left(\sqrt{\det\mathbf{C}^{e}}\right)\right) \tag{44a}$$

$$\psi_{i}^{kin}=\frac{c_{i}}{4}\left(tr\mathbf{C}_{i}^{pe}-3\right)-\frac{c_{i}}{2}\ln\left(\sqrt{\det\mathbf{C}_{i}^{pe}}\right) \tag{44b}$$

where μ and Λ are the Lamé constants, and c_i is the kinematic hardening parameter.

Thus, the corresponding constitutive relations for $\mathbf{S}$ and $\mathbf{X}_i$ are derived

$$\mathbf{S}=\mu\left(\mathbf{C}^{p^{-1}}-\mathbf{C}^{-1}\right)+\frac{\Lambda}{2}\left(\det\mathbf{C}\left(\det\mathbf{C}^{p}\right)^{-1}-1\right)\mathbf{C}^{-1} \tag{45a}$$

$$\mathbf{X}_{i}=\frac{c_{i}}{2}\left(\mathbf{C}_{i}^{pi^{-1}}-\mathbf{C}^{p^{-1}}\right) \tag{45b}$$

It should be noted that Ohno-Kairm model reduces to A-F model when $u_i=1$, and reduces to Ohno-Wang model when $u_i=0$ in Eq. (39b), respectively.

3. Numerical examples

The prediction ability and stability of A-F model at finite deformations had been investigated [21-23]. In this section, some numerical examples were carried out under strain controlled and stress controlled cyclic loadings, respectively.

The material parameters adopted is shown as table 1(parameters of Q and b are set to be zero as without considering isotropic hardening).

Table 1. Material parameters used in the proposed model

N=11, E=202GPa, v=0.33, σ_y=240MPa, Q=200, b=2.5, u_i=0.2;
$\zeta^{(1)}$=4000, $\zeta^{(2)}$=1052.6, $\zeta^{(3)}$=396.8, $\zeta^{(4)}$=200.4, $\zeta^{(5)}$=93.5, $\zeta^{(6)}$=50.1, $\zeta^{(7)}$=32.7, $\zeta^{(8)}$=22.9, $\zeta^{(9)}$=16.8, $\zeta^{(10)}$=12.6, $\zeta^{(11)}$=1.0;
$r^{(1)}$=1.29, $r^{(2)}$=4.83, $r^{(3)}$=6.39, $r^{(4)}$=5.42, $r^{(5)}$=25.3, $r^{(6)}$=30.8, $r^{(7)}$=67.7, $r^{(8)}$=66.7, $r^{(9)}$=65.6, $r^{(10)}$=111.4, $r^{(11)}$=5.0 (*MPa*).

It should be noted here

$$c_i = \frac{2}{3}\zeta_i r_i\,, \quad b_i = \zeta_i \tag{46}$$

The strain and stress at finite deformation modeling is logarithmic strain (true strain) and Cauchy stress, i.e.

$$\boldsymbol{\varepsilon} = \ln \mathbf{V}\,, \quad \boldsymbol{\sigma} = \frac{1}{\det \mathbf{F}} \mathbf{F}\mathbf{S}\mathbf{F}^T \tag{47}$$

with

$$\mathbf{V} = \mathbf{F}\mathbf{F}^T \tag{48}$$

3.1. Cyclic straining

3.1.1. Uniaxial tension-compression

In the section, Capacity of the proposed model describing Bauschinger effect is investigated. For finite deformation modeling, it can be controlled by

$$\mathbf{F} = \begin{vmatrix} 1+\Delta & 0 & 0 \\ 0 & e & 0 \\ 0 & 0 & e \end{vmatrix}, \quad S_{22} = S_{33} = 0 \tag{49}$$

where Δ is the applied load, and the unknown e can be determined through Eq. (49).

The stress-strain curves (1 cycle, with $\Delta: 0 \to 0.6487 \to 0 \to 0.3935 \to 0$) are shown as follows:

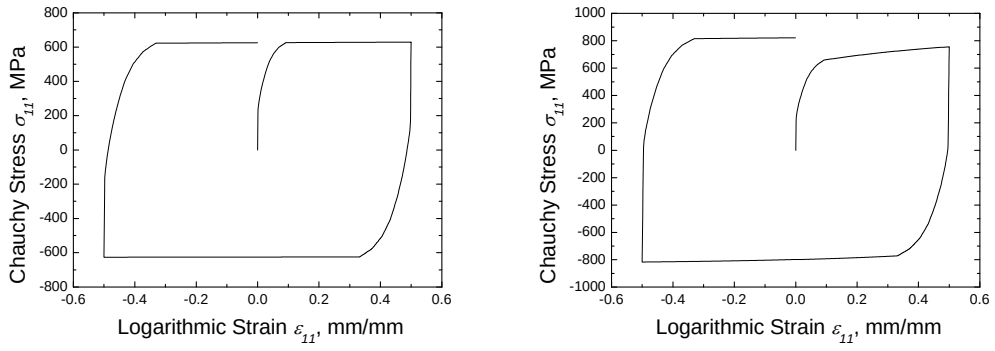

(a) (b)

Figure 2. Uniaxial tension-compression under cyclic straining: (a) without isotropic hardening, (b) with isotropic hardening.

Figure 2 shows the stress-strain curves in one loading cycle under strain controlled. It is found that Bauschinger effect in loading-unloading cycle is reasonably reproduced even though in a relative large strain regime (maximum strain is up to 64.87%). Comparing figure 2(a) and 2(b), it is shown that if isotropic hardening is considered, the strain hardening process can be well simulated.

3.1.2. Simple shear

When shear deformation is very large, shear oscillatory phenomenon will appear if the unreasonable finite deformation frame is adopted. It is very important to validate the prediction in shear deformation case for a developed model at finite deformations.

For simple shear case, deformation gradient can be expressed as

$$F = \begin{vmatrix} 1 & \lambda & 0 \\ 0 & 1 & 0 \\ 0 & 0 & e \end{vmatrix}, \quad S_{33} = 0 \tag{50}$$

where λ is the load, and the unknown e can be determined through Eq. (50).

The stress-strain curves (1 cycle, with $\lambda : 0 \to 0.5 \to 0 \to -0.5 \to 0$) are shown as follows:

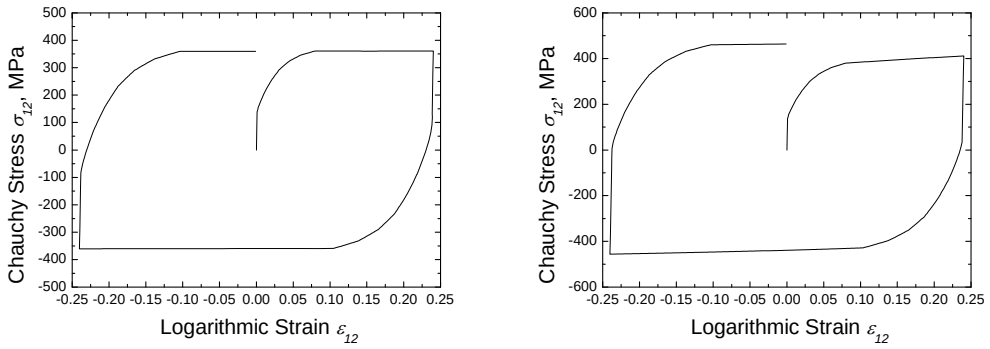

(a) (b)

Figure 3. Simple shear under cyclic straining: (a) without isotropic hardening, (b) with isotropic hardening.

It is shown from Figure 3 that no shear oscillatory phenomenon appears in simple shear case in a relative large strain regime, including with and without consider isotropic hardening cases.

3.2. Cyclic stressing

The prediction ability of ratchetting behaviour is investigated in this section. The loading cases are (150 ± 350)MPa and (100 ± 200)MPa for uniaxial tension-compression and simple shear cases, respectively. The stress-strain curves (10 cycles) are shown as follows:

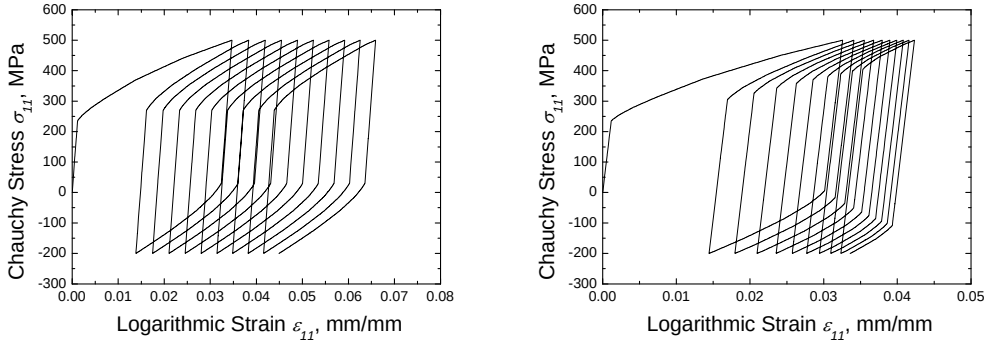

(a) (b)

Figure 4. Uniaxial tension-compression under cyclic stressing: (a) without isotropic hardening, (b) with isotropic hardening.

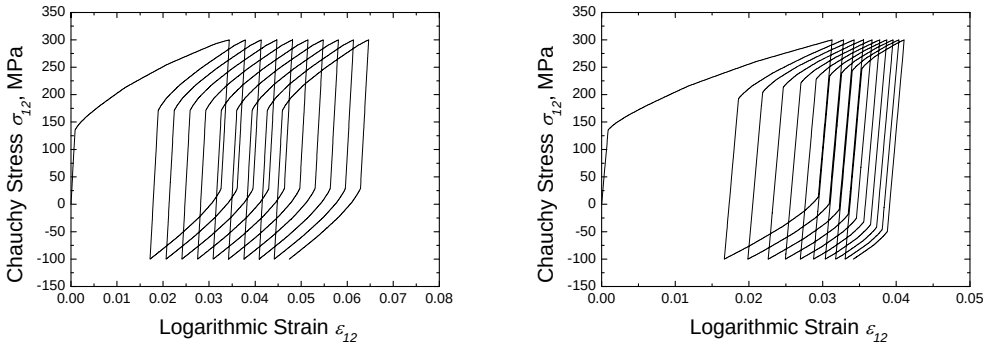

(a) (b)

Figure 5. Simple shear under cyclic stressing : (a) without isotropic hardening, (b) with isotropic hardening.

It is shown from Figure 4 that the presented model can reproduce ratchetting behaviour, regardless of uniaxial tension-compression or simple shear case. Moreover, the ratchetting strain exhibits a constant evolution rate without isotropic hardening; however, the evolution rate of ratchetting strain decreases as isotropic hardening is considered, which is a good agreement with constitutive models at small deformation [7].

4. Conclusions

Cyclic models at finite deformations were derived based on hyper-elastic theory. The deformation gradient is first additional multiplicatively decomposed into elastic and inelastic parts; inelastic part of deformation gradient is further decomposed into energetic and dissipative parts. Based on the frame of finite deformation, the cyclic constitutive model, combining isotropic hardening and Ohno-Karim nonlinear kinematic hardening rules, was proposed to describe Bauschinger effect and ratchetting behaviour. The proposed constitutive equations had been proven to satisfy Clausius-Duhem inequality. Tension-compression and simple shear simulations under cyclic stressing and straining were performed to validate the proposed model.

Acknowledgements

This work was supported by the Doctoral Innovation Funds of Southwest Jiaotong University (2013) and the Fundamental Research Funds for the Central Universities (SWJTU12CX044).

References

[1] C.O. Fredericka, P.J. Armstrong, A mathematical representation of the multiaxial Bauschinger effect. Tech. Rep. RD/B/N731, Berkeley Nuclear Laboratories, 1966.
[2] J.L. Chaboche, Time-independent constitutive theories for cyclic plasticity. Int. J. Plasticity, 2(1986) 149-188.
[3] J.L. Chaboche, Constitutive equations for cyclic plasticity and cyclic viscoplasticity. Int. J. Plasticity, 5(1998) 247-302.
[4] J.L. Chaboche, A review of some plasticity and viscoplasticity constitutive theories. Int. J.

Plasticity, 24(2008) 149-188.
[5] N. Ohno , J.D. Wang, Kinimatic hardening rules with critical state of dynamic recovery, Part I: Fornulation and basic features for ratchetting behavior. Int. J. Plasticity, 9(1993) 375-391.
[6] N. Ohno, J.D. Wang, Kinimatic hardening rules with critical state of dynamic recovery, Part II: Application to experiments of ratchetting behavior, Int. J. Plasticity, 9(1993) 391-403.
[7] M. Abdel-Karim, N. Ohno, Kinematic hardening model suitable for ratchetting with steady -state. Int. J. Plasticity, 16(2000) 225-240.
[8] M. Abdel-Karim, Numerical integration method for kinematic hardening rules with partial activation of dynamic recovery term. Int. J. Plasticity, 21(2005) 1303-1321
[9] G.Z. kang, N. Ohno, A. Nebu, Constitutive modeling of strain-range-dependent cyclic hardening. Int. J. Plasticity, 19(2003) 1801-1819.
[10] C. Tsakmakis, Kinematic hardening rules at finite plasticity, Part 1: a constitutive approach. Continuum Mech. Thermodynam, 8(1996) 215-231.
[11] C. Tsakmakis, Kinematic hardening rules at finite plasticity, Part 2: some examples. Continuum Mech. Thermodynam, 8(1996) 233-246.
[12] C. Tsakmakis, A. Willuweit, A comparative study of kinematic hardening rules at finite deformations. International Journal of Non-Linear Mechanics, 39(2004) 539-554.
[13] G. Lührs, On the numerical treatment of finite deformations in elastoviscoplasticity, Comput. Methods Appl. Mech. Engrg, 144(1997) 1-21.
[14] B. Svendsen, S. Arndt, D. Klingbeil, R. Sievert, Hyperelastic models for elastoplasticity with nonlinear isotropic and kinematic hardening at large deformation, Int. J. Solids Struct, 35 (1998) 3363-3389.
[15] A. Lion, Constitutive modelling at finite thermoviscoplasticity: a physical approach based on nonlinear rheological models. Int. J. Plasticity, 16(2000) 469-494.
[16] F. Mollica, K.R. Rajagopal, A.R. Srinivasa, The inelastic behavior of metals subject to loading reversal, Int. J. Plast, 17(2001) 1119-1146.
[17] L.J. Shen, Constitutive relations for isotropic or kinematic hardening at finite elastic–plastic deformations. Int. J. Solids Struct, 43(2006) 5613-5627.
[18] O.T. Bruhns, H. Xiao, A. Meyers, Self-consistent Eulerian rate type elasto-plasticity models based upon the logarithmic stress rate. Int. J. Plasticity, 15(1999) 479-520.
[19] O.T. Bruhns, H. Xiao, A. Meyers, Large simple shear and torsion problems in kinematic hardening elasto-plasticity with logarithmic rate. Int. J. Solids Struct, 38(2001) 8701-8722.
[20] H. Xiao, O.T. Bruhns, A. Meyers, A consistent finite elastoplasticity theory combining additive and multiplicative decomposition of the stretching and the deformation gradient. Int. J. Plasticity, 16(2000) 43-177.
[21] A.V. Shutov, R. Kreißig, Finite strain viscoplasticity with nonlinear kinematic hardening: Phenomenological modeling and time integration. Comput. Methods Appl. Mech. Engrg, 197 (2008) 2015-2029.
[22] W. Dettmer, S. Reese, On the theoretical and numerical modeling of Armstrong-Frederick kinematic hardening in the finite strain regime. Comput. Methods Appl. Mech. Engrg, 193 (2004) 87-116.
[23] I.N. Vladimirov, M.P. Pietryga, S. Reese, On the modelling of non-linear kinematic hardening at finite strains with application to springback-Comparison of time integration algorithms. Int. J. Numer. Meth. Engng 75(2008) 1-28.
[24] D.L. Henann, L. Anand, A large deformation theory for rate-dependent elastic-plastic materials with combined isotropic and kinematic hardening. Int. J. Plasticity, 25(2009) 1833-1878.
[25] E. Kröner, Allgemeine kontinuumstheorie der versetzungen und eigenspannungen. Archive for Rational Mechanics and Analysis 4(1960) 273-334.
[26] J.C. Simo, K.S. Pister, Remarks on rate constitutive equations for finite deformation problem: computational implications. Compt. Meth. Appl. Mech. Engng, 46(1984) 201-215.